Determination of the drag coefficient of finite cylinder at moderate Reynolds number and its implementation for simulation of fibre behaviour

Grzegorz Kondora, Dariusz Asendrych

Institute of Thermal Machinery
Czestochowa University of Technology
Poland

Plan of the presentation

1. **Introduction and motivation**
   - Lagrangian fibre model
   - Drag models
2. **CFD model**
   - Setup
   - Verification
3. **Results**
   - Comparison with Stokes drag
   - Single segment, aligned with the flow
   - Single element, perpendicular with the flow
   - Fibre
4. **Summary**

Introduction

and

motivation

Modelling methods of fibre suspension

single-phase approach

<u>rheology model</u>
<u>(data from experiment)</u>

$$\mu = f(\gamma)$$

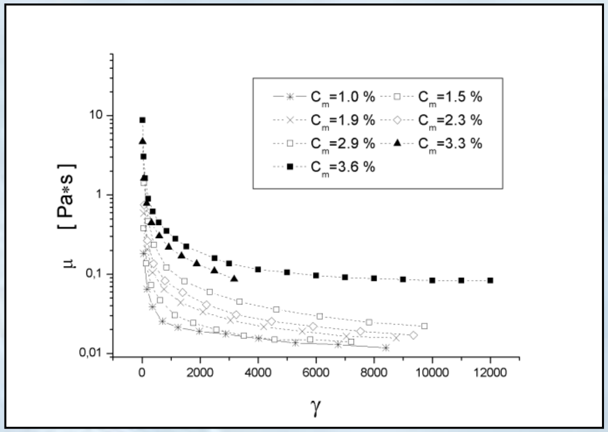

- useful only when pulp hydraulics is concerned
- experimental input needed

two-phase approach

<u>Eulerian (statistical)</u>

$$D_i \frac{\partial \Psi}{\partial x_i} - D_{ij} \frac{\partial^2 \Psi}{\partial x_j^2} = 0$$

$$\Psi = \Psi\left(x_i, \phi, \theta\right)$$

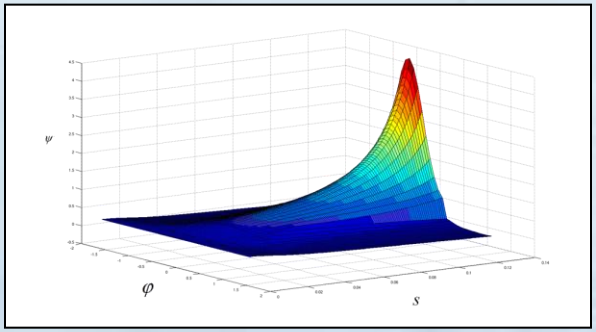

- valid for low consistencies (no fibre- fibre contact included)
- low computational power demand

<u>Lagrangian (particle-level)</u>

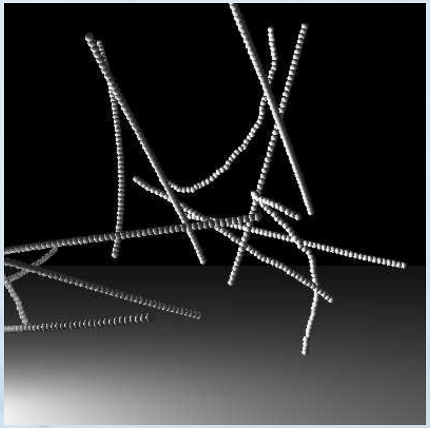

- deterministic model based on the physical laws
- huge computer resources needed

Lagrangian fibre model

- aim of my PhD thesis is to model fibre suspension flow in papermachine headbox
- in Lagrangian approach particles are treated as the **distinct entities** suspended in the fluid phase
- fibre model is made up of N_{seg} rigid **segments** connected by **ball** and socket **joints**

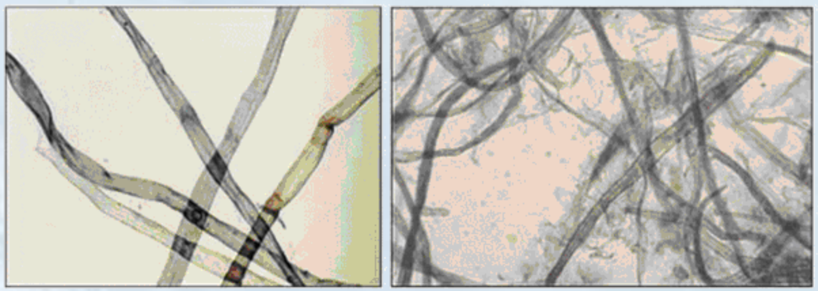

real cellulose fibres

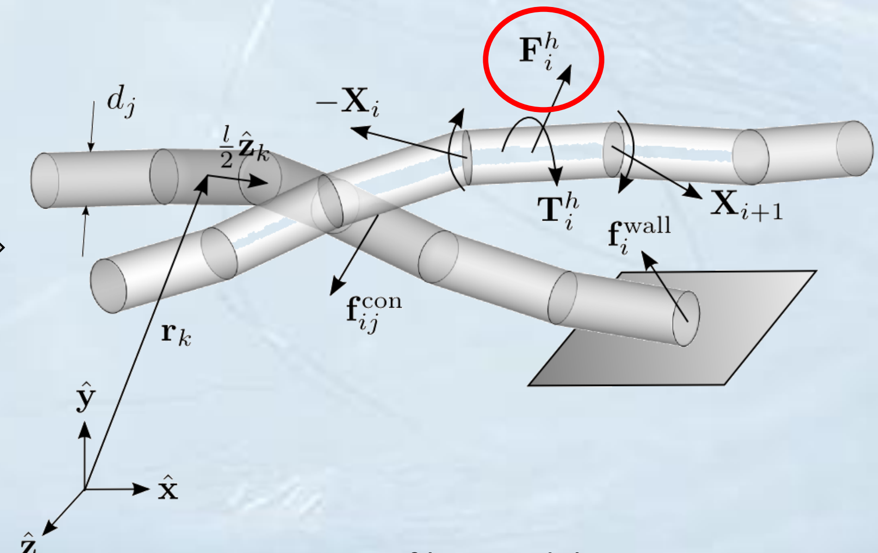

Lagrangian fibre model

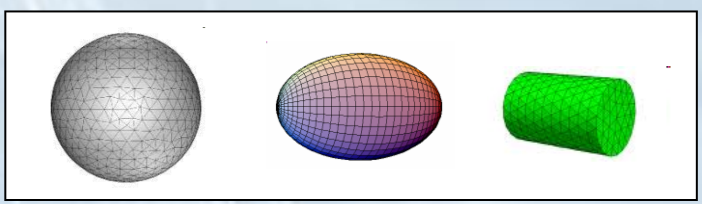

geometrical objects which may be used to represent fibre segment

adequate modelling of the hydrodynamic torque

Governing equations

direct application of Newton's second law for a fibre ith segment leads to:

$$m_p \ddot{\boldsymbol{r}}_i = \boldsymbol{F}_i^h - \boldsymbol{X}_i + \boldsymbol{X}_{i+1}$$

conservation of angular momentum on ith segment leads to:

$$\frac{\partial}{\partial t}(\boldsymbol{I}_i \cdot \boldsymbol{\omega}_i) = \boldsymbol{T}_i^h + \left(-\frac{l}{2}\hat{\mathbf{z}}_i\right) \times (-\boldsymbol{X}_i) + \frac{l}{2}\hat{\mathbf{z}}_{i+1} \times \boldsymbol{X}_{i+1} - \boldsymbol{Y}_i + \boldsymbol{Y}_{i+1}$$

connectivity equation:

$$\mathrm{f}_i(\boldsymbol{r}_i, \boldsymbol{z}_i) = \boldsymbol{r}_i + \frac{l}{2}\boldsymbol{z}_i - \left(\boldsymbol{r}_{i+1} - \frac{l}{2}\boldsymbol{z}_{i+1}\right) = \boldsymbol{0}$$

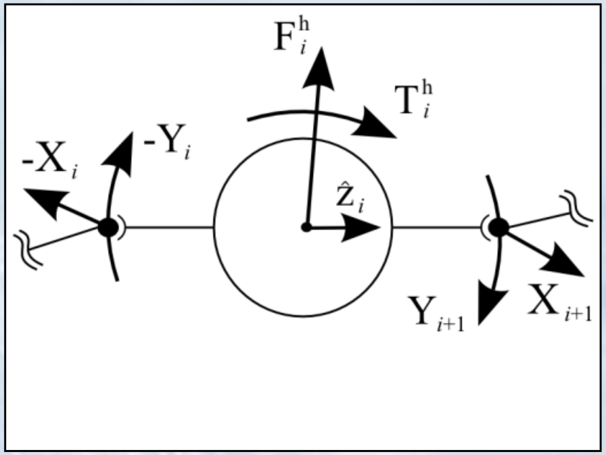

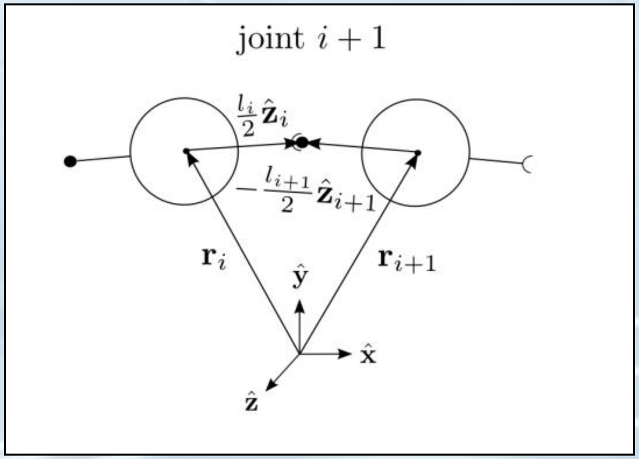

Particle Reynolds number

- typical fibre diameters: d = 20 ÷ 40 μm
- typical fibre length: L = 300 ÷ 3000 μm

$$\mathrm{Re}_p = \frac{\rho u_r D}{\mu} \qquad u_r = \left| u_f - u_p \right|$$

accroding to Vakil and Green [1] Re_p in papermaking is up to 60

according to Lindström [2] in headbox: $u_r \propto \frac{uL^2}{d^2}$

assuming that fluid structure has the same size as the thickness of the jet (1 cm), then:

$$u_r \approx \frac{1}{10} u_f$$

in modern headboxes: $u_f = 30 \quad m/s$, thus in the worst case (d = 30 μm, L = 3000 μm):

$$\mathrm{Re}_p = 100 \qquad \mathrm{Re} = 300\ 000$$

[1] Vakil A., Green S. I. - Drag and lift coefficients of inclined finite circular cylinders at moderate Reynolds numbers, *Computers & Fluids*, 2009
[2] Lindström S., Modellig and simulation of paper structure development, doctoral thests, Mid Sweden University, 2008

Drag models - sphere

<u>sphere-based fibre model</u>

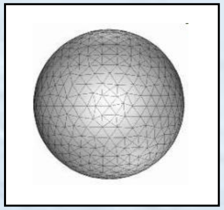

<u>Stokes drag</u> ($\mathrm{Re}_p \ll 1$)

hydrodynamic force and torque:

$$\mathbf{F}_i^h = \mathbf{A}_i^h \cdot \left(\mathbf{U}_f(\mathbf{r}_i) - \dot{\mathbf{r}}_i\right) \qquad \mathbf{M}_i^h = \mathbf{C}_i^h \cdot \left(\mathbf{\Omega}_f(\mathbf{r}_i) - \mathbf{\Omega}_i\right)$$

where resistance tensors are given as:

$$\mathbf{A}_i^h = 3\pi\mu d\boldsymbol{\delta} \qquad C_i^h = 4\pi\mu d^3\boldsymbol{\delta}$$

more often hydrodynamic force is given in the following form:

$$\mathbf{F}_i^h = \frac{1}{2}\rho A C_D \cdot \left(\mathbf{U}_f(\mathbf{r}_i) - \dot{\mathbf{r}}_i\right)\left|\mathbf{U}_f(\mathbf{r}_i) - \dot{\mathbf{r}}_i\right| \qquad C_D = \frac{\mathbf{F}_i^h}{\frac{1}{2}\rho\left(\mathbf{U}_i^r\right)^2 A} = \frac{24}{\mathrm{Re}_{p,i}}$$

<u>non-linear drag</u> ($\mathrm{Re}_p > 1$) – Morsi and Alexander [3] empirical drag law

$$C_D = a_1 + \frac{a_2}{\mathrm{Re}} + \frac{a_3}{\mathrm{Re}^2}$$

$$a_1,\ a_2,\ a_3 = \begin{cases} 0,\ 24,\ 0 & 0 < \mathrm{Re} < 0.1 \\ 3.690,\ 22.73,\ 0.0903 & 0.1 < \mathrm{Re} < 1 \\ 1.222,\ 29.1667,\ -3.8889 & 1 < \mathrm{Re} < 10 \\ 0.6167,\ 46.50,\ -116.67 & 10 < \mathrm{Re} < 100 \\ 0.3644,\ 98.33,\ -2778 & 100 < \mathrm{Re} < 1000 \\ 0.357,\ 148.62,\ -47500 & 1000 < \mathrm{Re} < 5000 \\ 0.46,\ -490.546,\ 578700 & 5000 < \mathrm{Re} < 10000 \\ 0.5191,\ -1662.5,\ 5416700 & \mathrm{Re} \geq 10000 \end{cases}$$

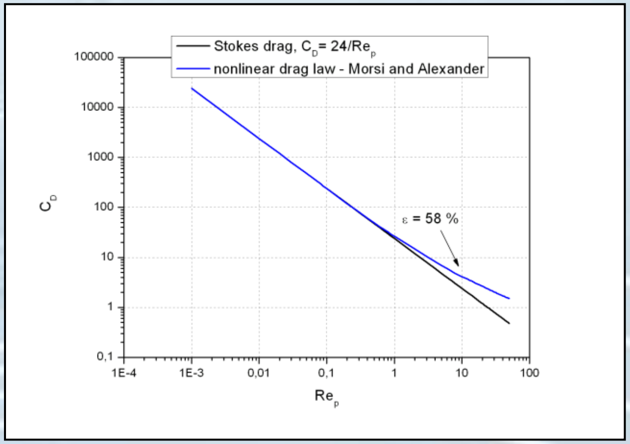

[3] Morsi S. A. and Alexander A. J., An Investigation of Particle Trajectories in Two-Phase Flow Systems, *Journal of Fluid Mechanics*, 1972

Drag models – prolate spheroid

prolate spheroid fibre model

extension of Stokesian drag for prolate spheroid oriented with vector z with respect to the flow direction:

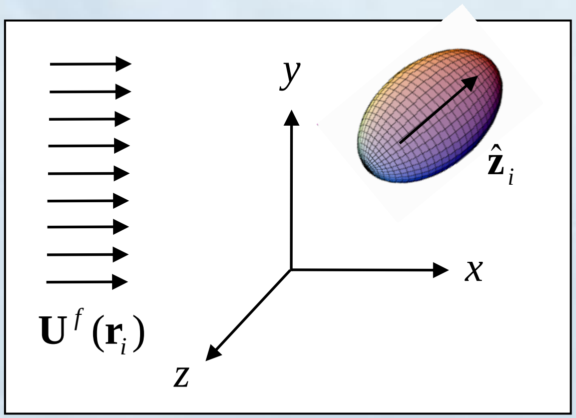

$$\mathbf{F}_i^h = \mathbf{A}_i^h \cdot \left(\mathbf{U}_f(\mathbf{r}_i) - \dot{\mathbf{r}}_i\right)$$

$$\mathbf{M}_i^h = \mathbf{C}_i^h \cdot \left(\boldsymbol{\Omega}_f(\mathbf{r}_i) - \boldsymbol{\Omega}_i\right) + \tilde{\mathbf{H}}_i^h : \mathbf{E}_f(\mathbf{r}_i)$$

$\mathbf{A}_i^h$	$3\pi\mu a\left[X^A \mathbf{z}_i\mathbf{z}_i + Y^A(\boldsymbol{\delta} - \mathbf{z}_i\mathbf{z}_i)\right]$ $X^A = \frac{8}{3}e^3\left[-2e + (1+e^2)\ln\left(\frac{1+e}{1-e}\right)\right]^{-1}$ $Y^A = \frac{16}{3}e^3\left[2e + (3e^2-1)\ln\left(\frac{1+e}{1-e}\right)\right]^{-1}$
$\mathbf{C}_i^h$	$\pi\mu a^3\left[X^C \mathbf{z}_i\mathbf{z}_i + Y^C(\boldsymbol{\delta} - \mathbf{z}_i\mathbf{z}_i)\right]$ $X^C = \frac{4}{3}e^3\left(1-e^2\right)\left[2e - (1-e^2)\ln\left(\frac{1+e}{1-e}\right)\right]^{-1}$ $Y^A = \frac{4}{3}e^3\left(2-e^2\right)\left[-2e + (1+e^2)\ln\left(\frac{1+e}{1-e}\right)\right]^{-1}$
$\tilde{\mathbf{H}}_i^h$	$-\pi\mu a^3 Y^H \boldsymbol{\varepsilon}\cdot\mathbf{z}_i\mathbf{z}_i$ $Y^H = \frac{4}{3}e^5\left[-2e + (1+e^2)\ln\left(\frac{1+e}{1-e}\right)\right]^{-1}$

no data for higher Re – use of cylinders instead of spheroids seems to be more natural choice – easier collision implementation

[4]Kim S., Karrila S. J., Microhydrodynamics: Principles and selected applications. Butterworth-Heineman, 1991

CFD simulation of flow around finite cylinder

CFD model

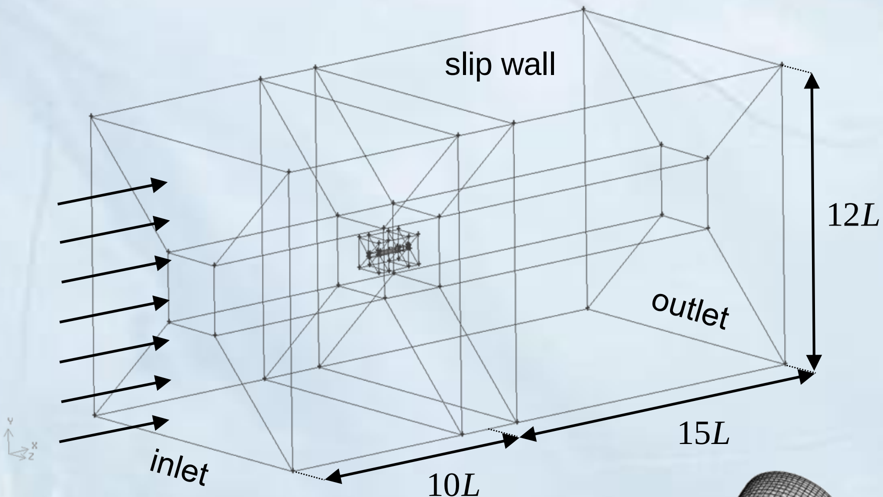

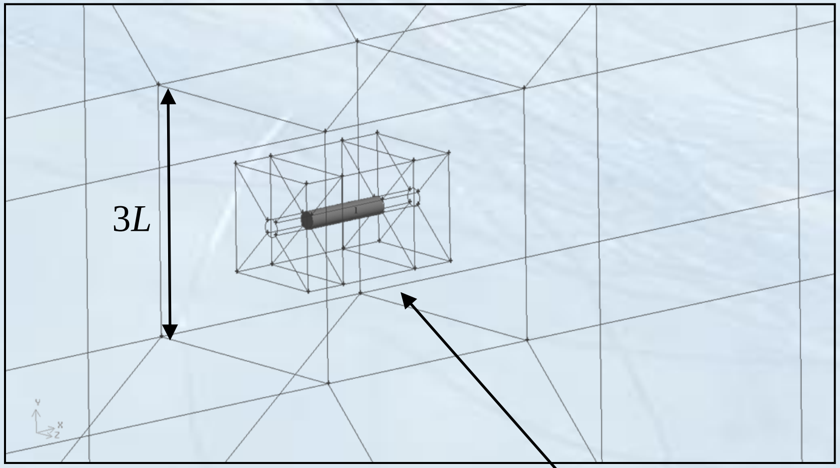

rotating box (hexcore mesh)

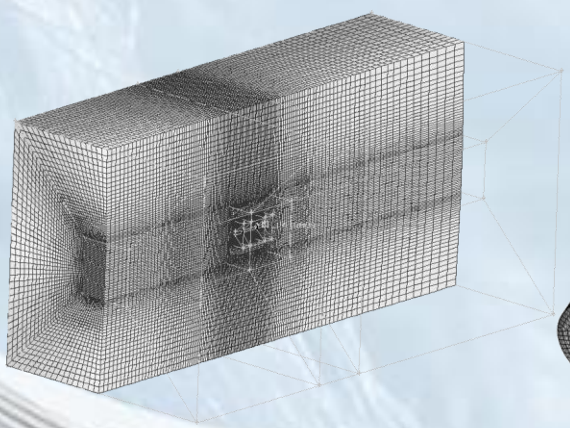

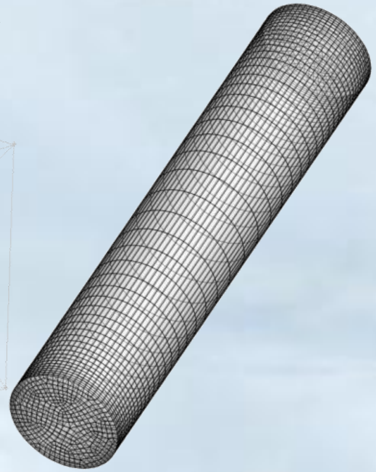

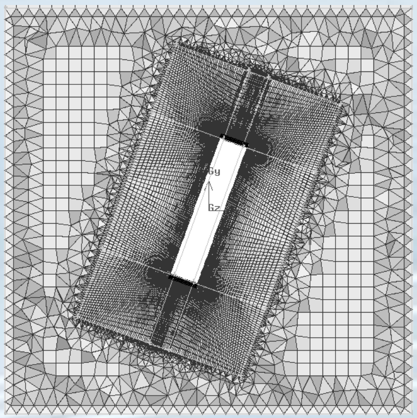

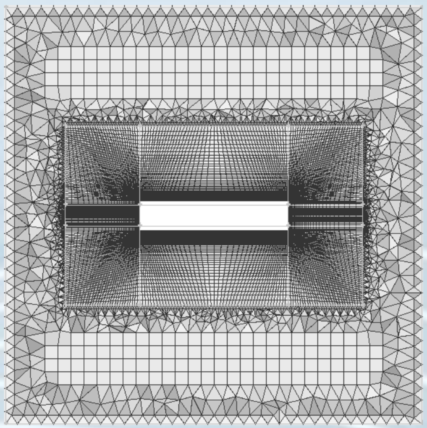

Calculation procedure

Perl script

```
…
…
for (Re = Re_start; Re <= Re_end; Re += Re_delta)
{
 for (theta = theta_start; theta <= theta_end; theta += Re_delta)
 {
  for (phi = phi_start; phi <= (90 – theta); phi += phi_delta)
  {
   run_gambit;
   run_fluent;
   postprocess;
  }
 }
}
…
…
```

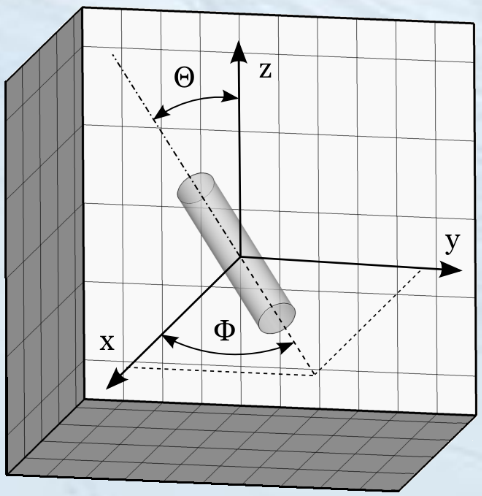

GAMBIT

- automatic mesh generation for given orientation with the use of journal files
- hexahedral in great part of the domain
- boundary layer applied near cylinder walls
- hexcore mesh used in rotating box
- typical mesh size – 2.3 million of cells

FLUENT

- performing simulation for given Re using mesh generated by GAMBIT
- second order discretization
- script for monitoring C_D convergence ($\varepsilon = 0.0001$)
- typical calculation for one case - 2 h (8 cores Intel Xeon …)
- total time (46 * 12 * 2 = 1104 h = 46 days)

Verification

mesh sensitivity tests performed on the sphere due to lack of experimental data needed to verify simulation:

- Re = 100 (steady axisymmetric regime 20 < Re < 210)
- variable denisty of boundary layer and mesh near the sphere
- after tests same boundary layer scheme applied on cylinder

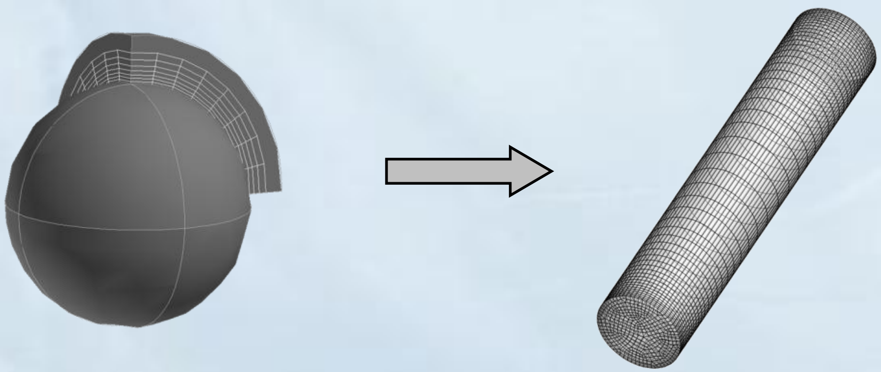

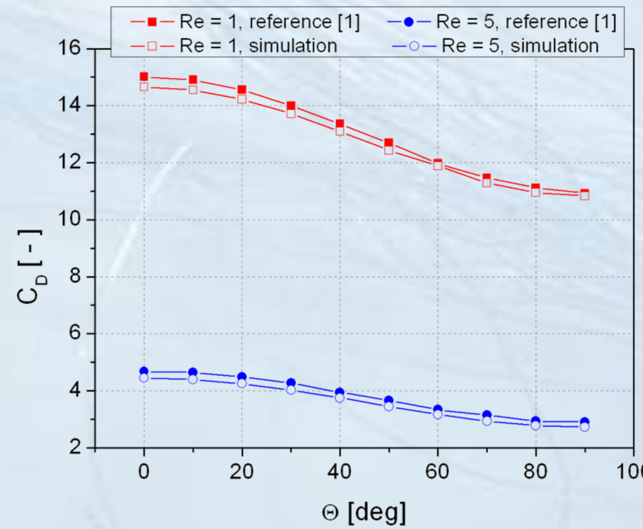

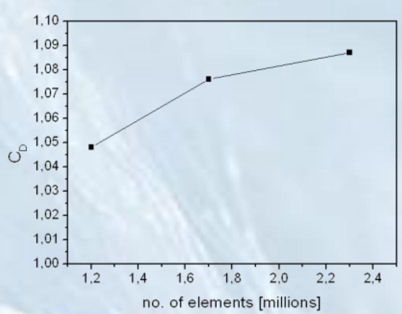

FLUENT: $C_D = 1.092$

literature: $C_D = 1.087 \div 1.096$

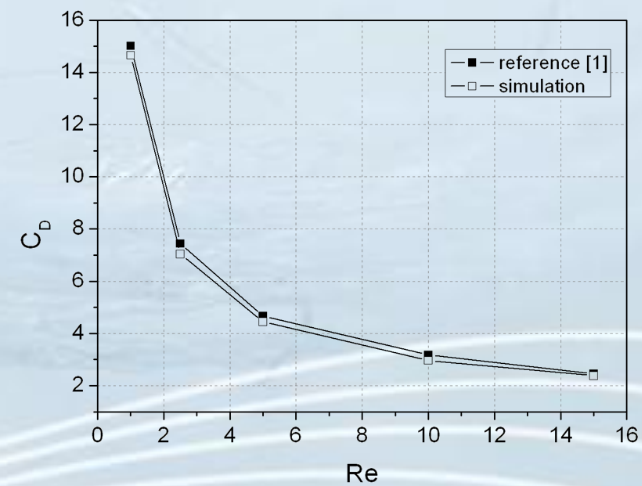

[1] Vakil A., Green S. I. - Drag and lift coefficients of inclined finite circular cylinders at moderate Reynolds numbers, *Computers & Fluids*, 2009

Results

Results

$$\mathbf{U}^r = \frac{\mathrm{Re}\,\mu}{\rho d} \qquad \mathbf{F}_{Stokes} = \mathbf{A}^h \cdot \mathbf{U}^r \qquad C_{D,Stokes} = \frac{\mathbf{F}_{Stokes}}{\frac{1}{2}\rho\left(\mathbf{U}^r\right)^2 A_{spheroid}} \qquad C_{D,FLUENT} = \frac{\mathbf{F}_{FLUENT}}{\frac{1}{2}\rho\left(\mathbf{U}^r\right)^2 A_{cylinder}} \qquad A_{spheroid} = \pi \frac{L}{2}\frac{d}{2}$$

$$A_{cylinder} = Ld$$

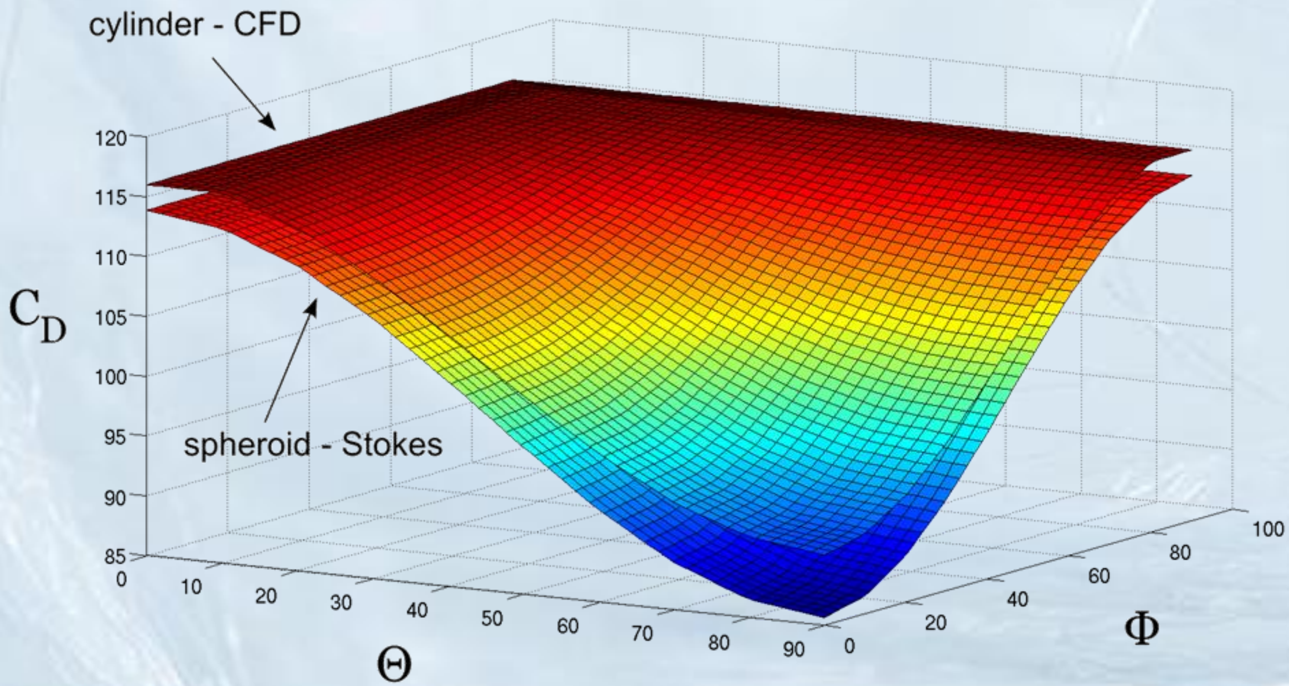

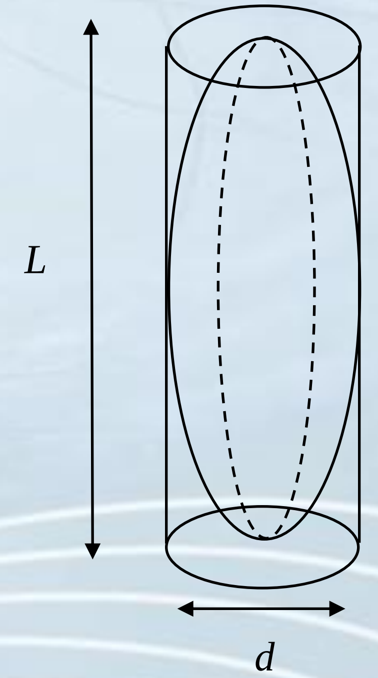

$\mathrm{Re} = 0.1$

Results

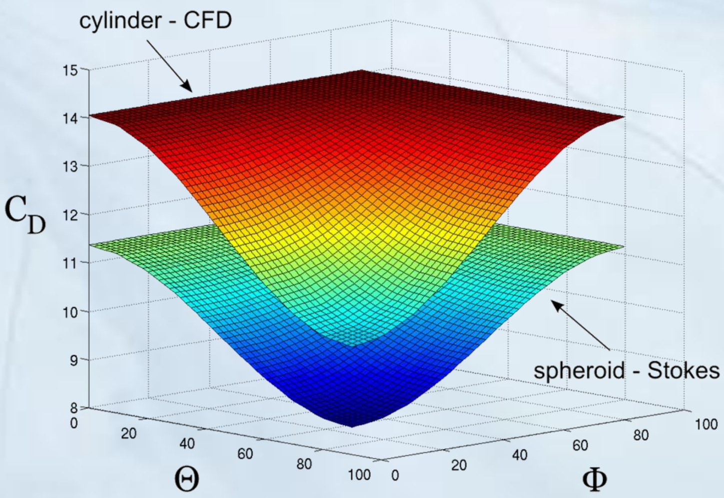

$\mathrm{Re} = 1.0$

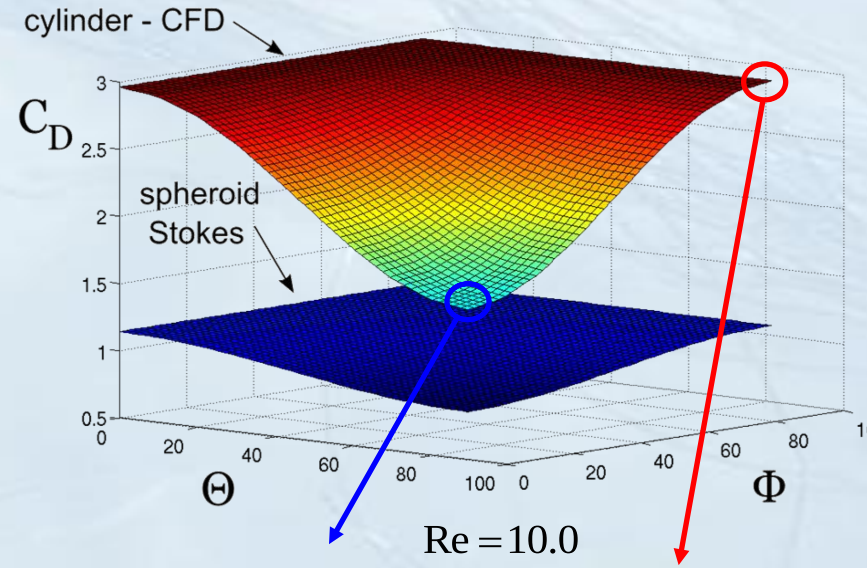

$\mathrm{Re} = 10.0$

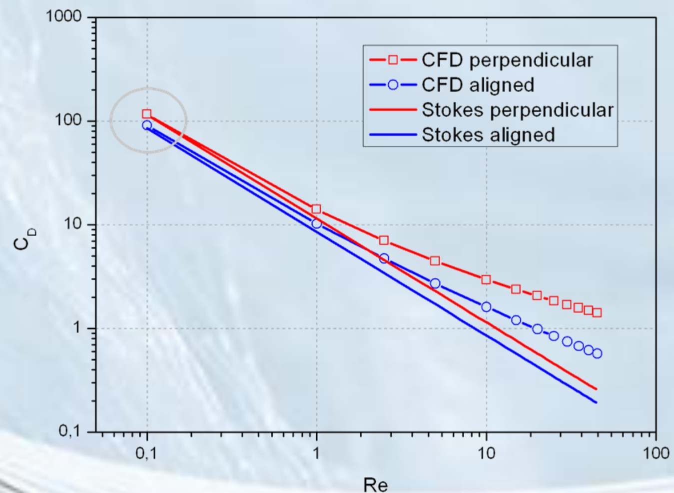

aligned with the flow

perpendicular to the flow

Flow field

simplified headbox flow – one-dimensional flow esspecialy at the centre line $y=0$ [4]

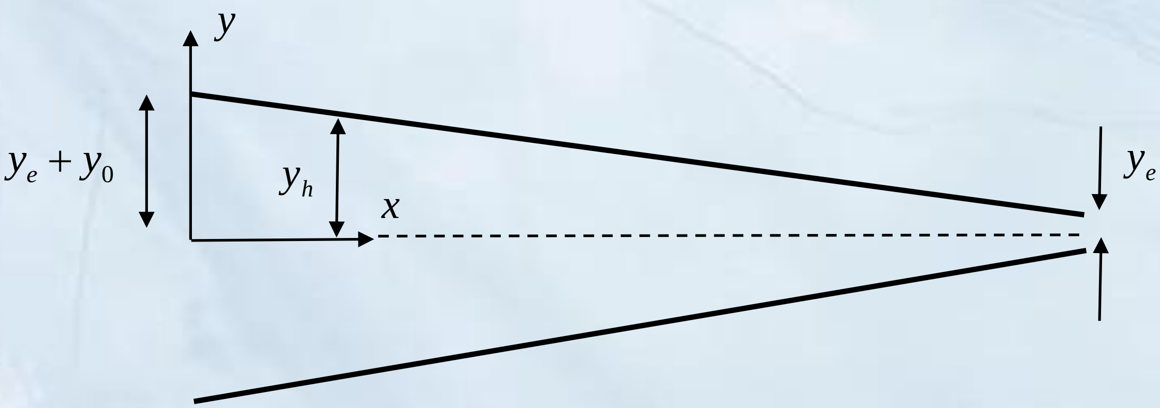

$$y_h = y_e + y_0 - y_0\left(\frac{x}{L}\right)^a$$

$$u(x)2y_h = const$$

$$u(x) = \frac{u(0)}{1-\left(1-\frac{1}{R}\right)\left(\frac{x}{L}\right)^a}$$

Why such a velocity field has been chosen for a test case???

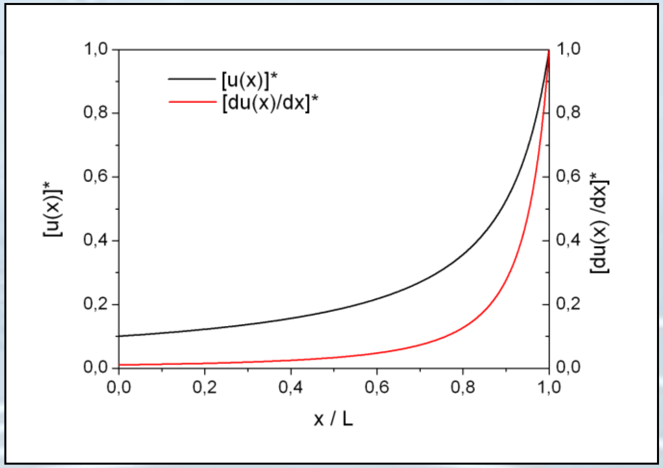

fibre aligned with the flow – no net hydrodynamic torque on every segment – its influence eliminated:

$$\mathbf{F}_i^h = \mathbf{A}_i^h \cdot \left(\mathbf{U}_f(\mathbf{r}_i) - \dot{\mathbf{r}}_i\right)$$

$$\mathbf{M}_i^h = \underbrace{\mathbf{C}_i^h \cdot \left(\mathbf{\Omega}_f(\mathbf{r}_i) - \mathbf{\Omega}_i\right) + \widetilde{\mathbf{H}}_i^h : \mathbf{E}_f(\mathbf{r}_i)}_{0}$$

[4] Olson J.A. S. A., Analytic estimate of the fibre orientation distribution in a headbox flow, *Nordic Pulp and Paper Research*, 2002

single element, aligned with the flow

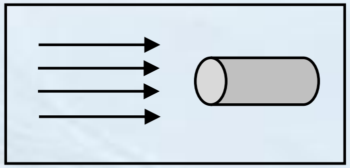

$d = 30\ \mu m \qquad L = 150\ \mu m$

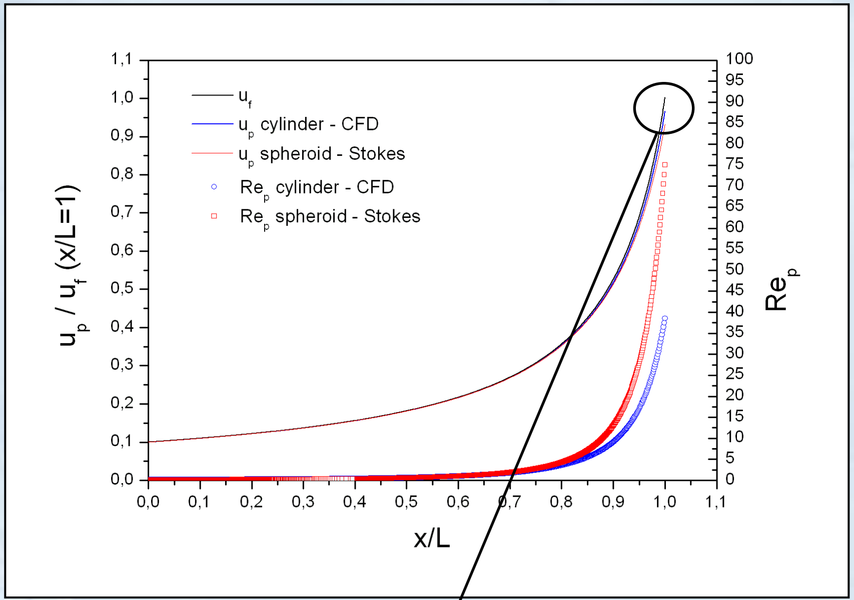

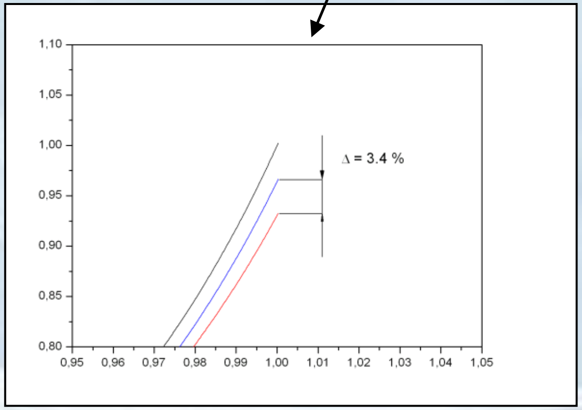

$d = 100\ \mu m \qquad L = 500\ \mu m$

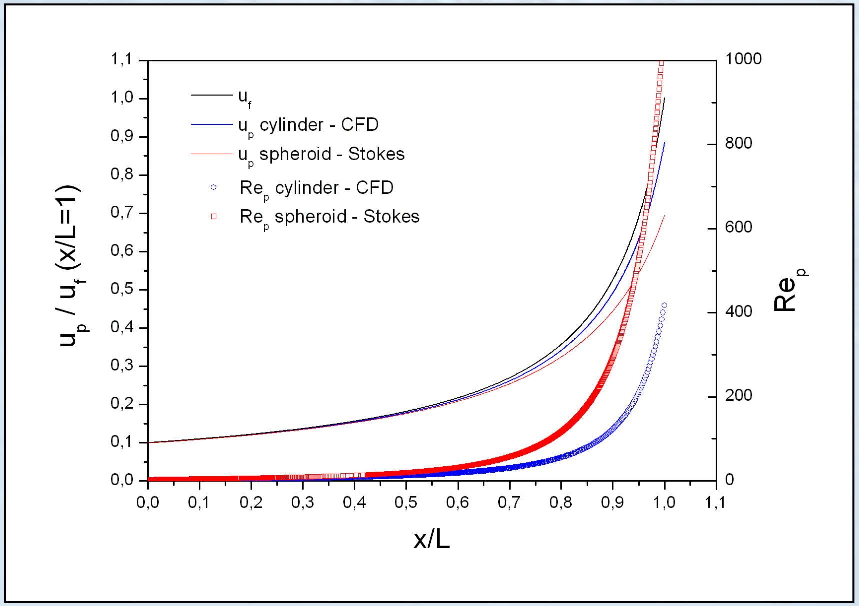

- small difference is seen between drag models for d = 30 µm – very low particle inertia – small Re due to small velocity difference
- when the size is inreased to 100 µm particle inertia is not negligible (Stokes number increased)

single element, perpendicular

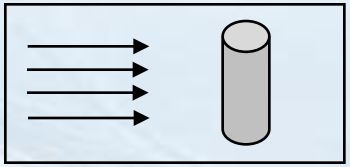

$d = 30\ \mu m \qquad L = 150\ \mu m$

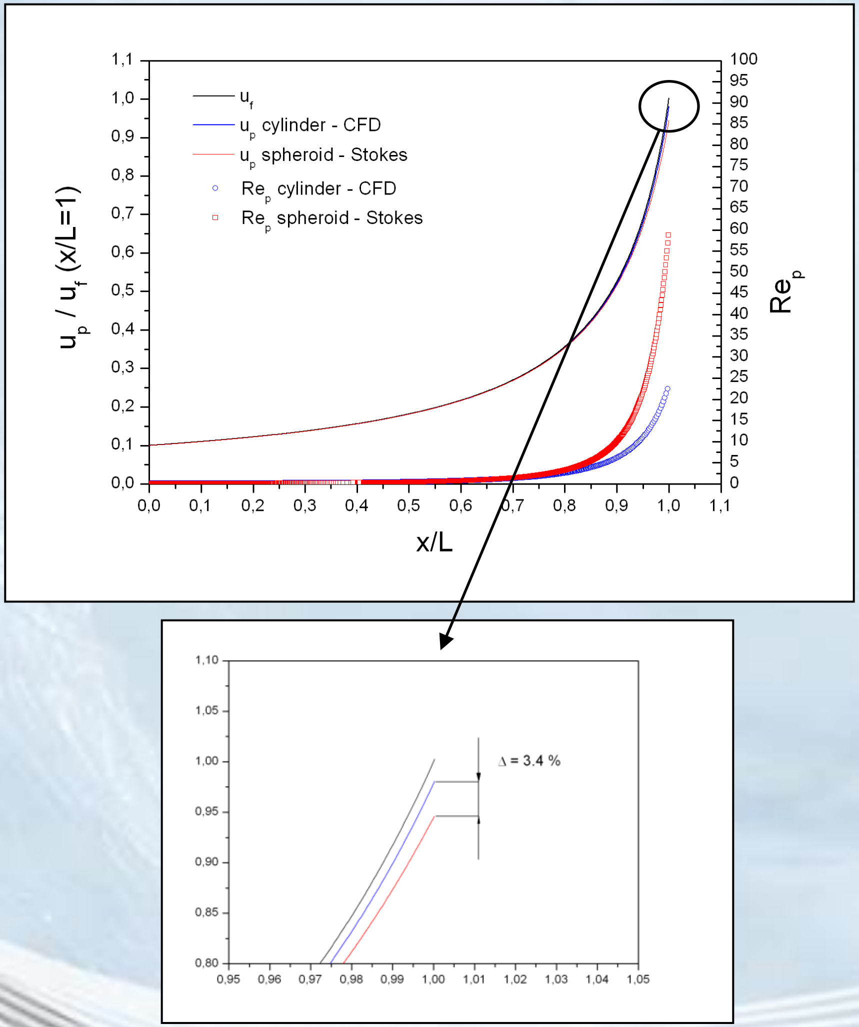

$d = 100\ \mu m \qquad L = 500\ \mu m$

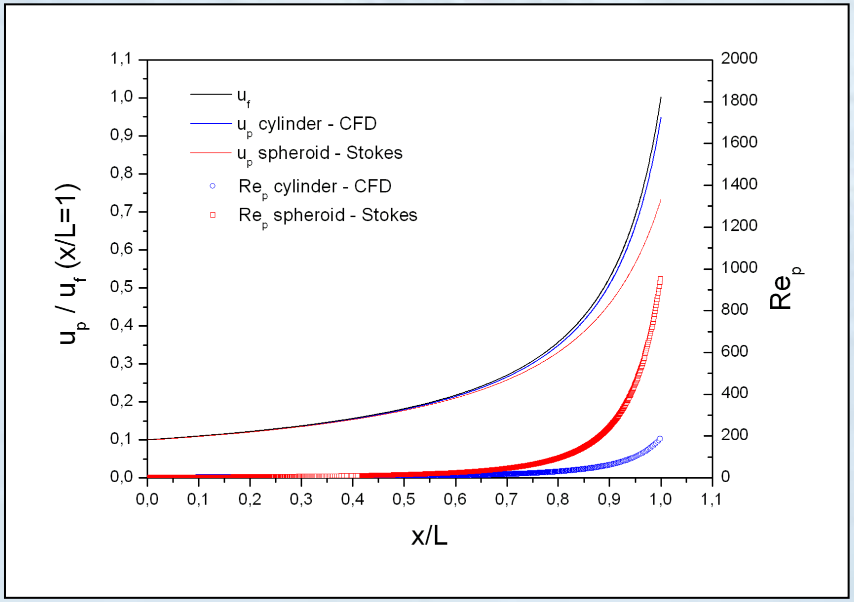

- same differences as for element aligned with the flow for smaller element diameter
- due to higher drag force cylinder with d = 100 µm moves almost wih the fluid velocity wheras Stokes law underestimate hydrodynamic resistance

fibre, aligned with the flow

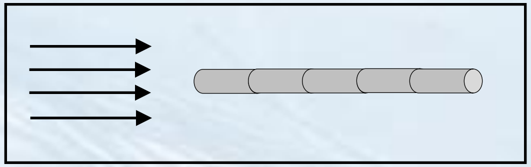

$d = 30\,\mu m \quad L = 3000\,\mu m \quad N_{seg} = 20$

$d = 100\,\mu m \quad L = 3000\,\mu m \quad N_{seg} = 6$

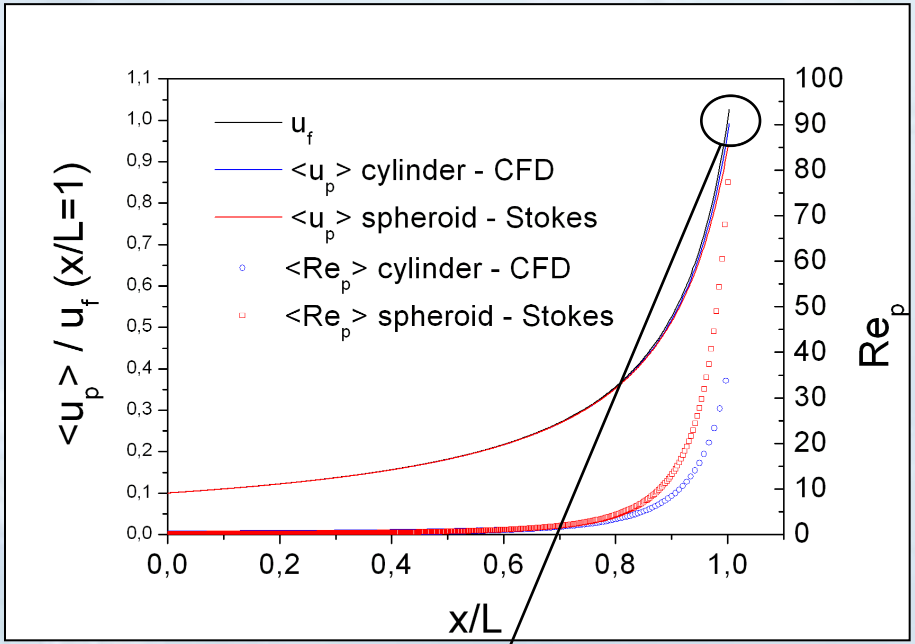

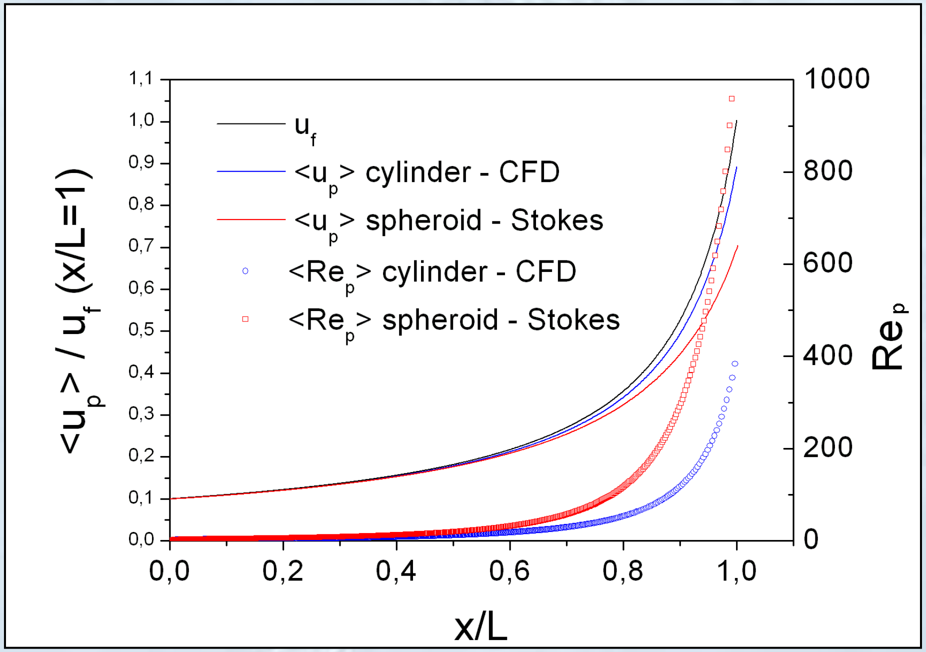

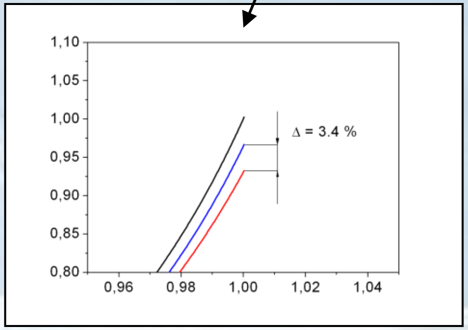

- relative error in velocity at the outlet for d = 30 μ between Stokes drag and predicted cylinder C_D is around 3.5 %
- for higher diamater and the same length inertial effect are more pronounced, every segment contributes to the total momentum balance

Summary

- CFD modelling technique was used to simulate flow around finite cylinder in order to determine hydrodynamic resistance in term of orientation angle, aspect ratio and Reynolds number

- simulation results compared to the drag function of prolate spheroid derived from Stokes flow by Kim and Karrila showed very good agreement for Re = 0.1 (upper limit of Stokes flow)

- for higher Re drag deviates from Stokes law (e.g. for Re = 10 relative error exceeds 55 %)

- in real flow situations:
  - ✓ velocity gradient field is three dimensional
  - ✓ there is a mechanical system of multiple interacting fibres
  - ✓ fibres are in contact with flow boundaries
  - ✓ turbulent fluctuations have to be taken into account

  thus Re may reach significantly higher values leading to more pronounced difference between Stokes and actually experienced drag

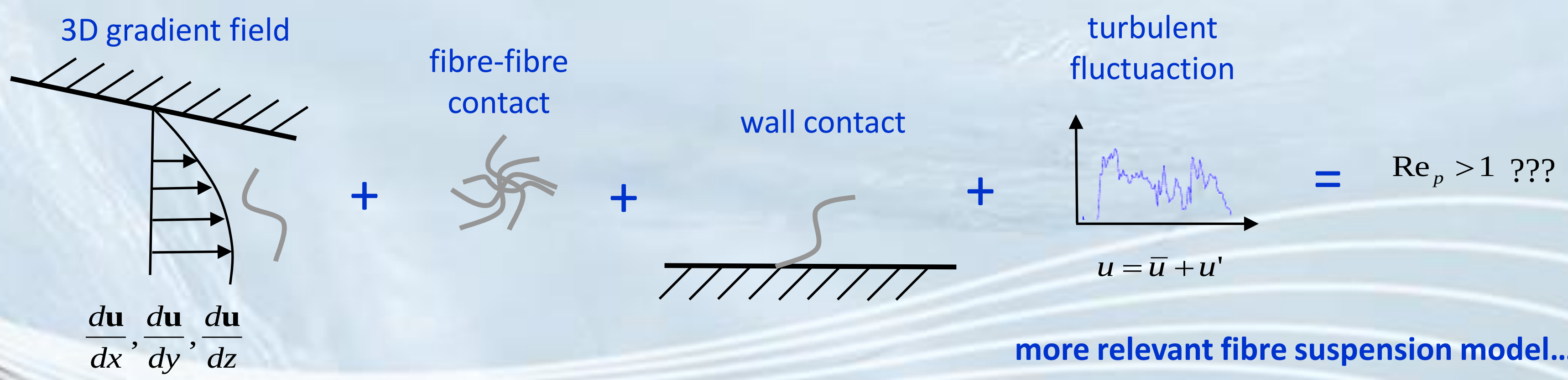

more relevant fibre suspension model…